Sensors and Actuators B 156 (2011) 169–175

Contents lists available at ScienceDirect

Sensors and Actuators B: Chemical

journal homepage: www.elsevier.com/locate/snb

Sensitivity comparison of surface plasmon resonance and plasmon-waveguide resonance biosensors

Abdennour Abbas, Matthew J. Linman, Quan Cheng*

Department of Chemistry, University of California, Riverside, CA 92521, USA

ARTICLE INFO

Article history:
Received 18 January 2011
Received in revised form 1 April 2011
Accepted 5 April 2011
Available online 12 April 2011

Keywords:
Optical biosensors
Surface plasmon resonance
Plasmon-waveguide resonance
Surface sensitivity
Planar waveguide

ABSTRACT

Plasmon-waveguide resonance (PWR) sensors are particularly useful for the investigation of biomolecular interactions with or within lipid bilayer membranes. Many studies demonstrated their ability to provide unique qualitative information, but the evaluation of their sensitivity as compared to other surface plasmon resonance (SPR) sensors has not been broadly investigated. We report here a comprehensive sensitivity comparison of SPR and PWR biosensors for the p-polarized light component. The sensitivity of five different biosensor designs to changes in refractive index, thickness and mass are determined and discussed. Although numerical simulations show an increase of the electric field intensity by 30–35% and the penetration depth by four times in PWR, the waveguide-based method is 0.5–8-fold less sensitive than conventional SPR in all considered analytical parameters. The experimental results also suggest that the increase in the penetration depth in PWR is made at the expense of the surface sensitivity. The physical and structural reasons for PWR sensor limitations are discussed and a general viewpoint for designing more efficient SPR sensors based on dielectric slab waveguides is provided.

1. Introduction

The development of new strategies for signal enhancement that leads to improved sensitivity and/or resolution has been a major issue for the surface plasmon resonance (SPR) community over the last decade. Currently, SPR is a well established technique for kinetic studies of biomolecular interactions. Considerable efforts have been taken to substantially enhance the performance and noticeable progress has been made in three important directions: sub-picomolar or trace analyte concentrations [1,2], low molecular weight substances (<500 Da) [3,4], and the most challenging of all, single molecule detection [5,6]. The major challenge in this research direction is to find new strategies to circumvent the intrinsic limitation of the traditional SPR substrates, particularly the penetration depth which is usually lower than 300 nm [7], while keeping the fabrication process relatively easy.

One of the promising strategies to improve the performance of SPR sensors is the generation of a guided mode in the SPR planar substrate. Coupling a waveguide mode to surface plasmon polaritons was first proposed by Macleod more than two decades ago [8]. The idea was later implemented by Salamon et al. who developed the first plasmon-waveguide resonance biosensor and extensively studied the applications in membrane systems [9,10]. Since then, many research groups proposed modified designs [11–14] and applied the concept to a variety of biological targets [15–17]. Plasmon-waveguide resonance is based on the deposition of a dielectric layer over a gold or silver film. To act as a waveguide at microwave or optical frequencies, this layer must satisfy some conditions, as described by Tien [18]. Many conductive or dielectric materials have been used in this purpose, particularly silica and titanium dioxides. The film thickness should be higher than the cut-off thickness, which is around $\lambda/2n$ where λ is the excitation wavelength and n is the refractive index of the material. Additionally, the film needs to be surrounded by two layers of lower refractive indices in order to enable the wave propagation by total internal reflection. In PWR sensors, one of the surrounding layers is generally glass/metal and the second is air or the medium to be analyzed (Fig. 1).

The role of the waveguide layer is primarily the generation of waveguide modes excited by either p- or s-polarized light. This mode is mostly confined in the bulk film. This property has inspired the use of porous waveguide films for analyte immobilization inside the pores and thus taking advantage of the high electromagnetic field intensity while increasing the analyte charge density [19,20]. Guided modes are highly sensitive to changes in the refractive index with both polarizations. This advantage is used to investigate the birefringence and optical dichroism of anisotropic materials such as lipid bilayer membranes, self assembled monolayers and thin films [10,12]. This is mainly achieved by dealing with four optical parameters (two refractive indices and two extinction coefficients)

* Corresponding author. Tel.: +1 951 827 2702; fax: +1 951 827 4713.
E-mail address: quan.cheng@ucr.edu (Q. Cheng).

0925-4005/$ – see front matter © 2011 Elsevier B.V. All rights reserved.
doi:10.1016/j.snb.2011.04.008

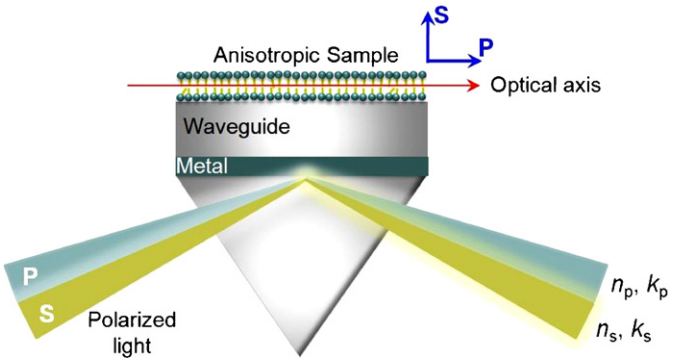

Fig. 1. Principle of plasmon-waveguide resonance biosensors.

rather than two in conventional SPR (Fig. 1). The combination of s- and p-spectral parameters can give access to the mass density and distribution which reflect the molecular order and conformation of anisotropic materials [10]. The waveguide layer has also the advantage of protecting and thus enabling the use of silver film, which is known to be highly resonant but chemically instable, although this protection function is limited when a porous film is used. In addition, silicon and titanium dioxides that are commonly used as waveguides display very good hydrophilicity, thus offering a suitable platform for lipid vesicle fusion and biomembrane analysis. Finally, coupling a waveguide mode to surface plasmons leads to the enhancement of the electric field as it will be discussed later.

Even though this hybrid biosensor has been widely used and the sensitivity of PWR and SPR sensors extensively but separately studied, there is currently no literature directly comparing both research avenues, especially in the angular scanning mode of detection. Considering the different instruments used by different authors and the variability of the optical parameters of the different materials involved, it is obvious that only a direct comparison with the same SPR instrument, same materials and experimental conditions can bring relevant information on the relative performance of each design.

Herein, we carried out the fabrication of five different SPR chips in a single process to ensure the same experimental conditions. The current study focused on the p-polarized light excitation. The optical parameters of these materials were determined and the distribution of the electromagnetic field through the multilayer system was obtained using 3-D finite-difference time-domain (FDTD) simulations. The sensitivity in the bulk solution, referred to as "bulk sensitivity", was experimentally determined using ethanol–water mixtures, followed by the evaluation of the sensitivity at the interface film/fluid, referred to as "surface sensitivity", using both lipid bilayer membrane deposition and biomolecular interactions. The results are compared to the theoretical predictions, and the improvement brought by each design is discussed along with the contribution of the different layers. Finally we discuss the reasons behind the limitation in PWR sensors sensitivity and suggest a new concept for future design improvement.

2. Experimental

2.1. Materials

The metals (gold, silver, chromium) used for electron-beam evaporation were acquired as pellets of 99.99% purity from Kurt J. Lesker (USA). Ethanol (200 proof) was obtained from Gold Shield Chemical Co. (USA). L-α-Phosphatidylcholine (PC) was purchased from Avanti Polar Lipids (Alabaster, AL). Cholera toxin (CT) from *Vibrio cholera* and Triton X-100 was obtained from Sigma–Aldrich (St. Louis, MO). The monosialoganglioside receptor (G_{M1}) was obtained from Matreya (Pleasant Gap, PA). All lipids were made into stock solutions in chloroform and stored in a −80 °C freezer unless otherwise noted.

2.2. Numerical modeling

Numerical modeling was performed using 3-D finite-difference time-domain (FDTD) method-based analysis with commercially available software (*EM Explorer*). FDTD methods exploit the time and position dependence of Maxwell's equations to model electromagnetic waves in rectangular 3D cells of finite volume. We modeled our structure by using Yee cell size of 0.02 μm, which is about 1/20th of the wavelength, giving an accuracy of 1–2%. The structure (4 μm × 3 μm × 3 μm) was illuminated with an incident plane wave (λ = 650 nm) with Perfectly Matched Layer (PML) absorbing boundary conditions. The optical param-

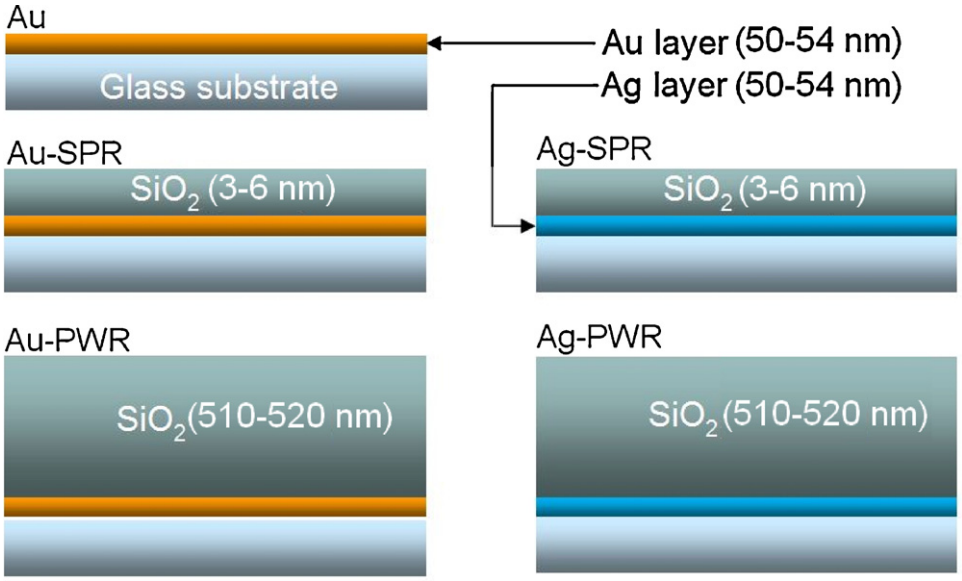

Fig. 2. Different biosensor designs used for sensitivity comparison experiments. Au-SPR and Ag-SPR represent conventional gold and silver SPR chips functionalized with 3–6 nm silicon dioxide. Au-PWR and Ag-PWR are plasmon-waveguide resonance chips using gold and silver respectively. Au is bare gold substrate.

eters and thickness (d) of gold ($\varepsilon = -14.81 + i0.76$, $d = 52.6$ nm), silver ($\varepsilon = -16.28 + i0.60$, $d = 53.5$ nm), chromium ($\varepsilon = 7.97 + i7.94$, $d = 2.2$ nm), silicon dioxide ($\varepsilon = 2.12$, $d = 510$ nm for PWR chips and 3.6 nm for SPR chips) were determined by fitting the theoretical reflectivity curves obtained by FDTD calculations with the experimental curves obtained using the NanoSPR6 spectrometer.

2.3. Biosensor fabrication

The fabrication process was carried out using the electron-beam evaporator Temescal BJD 1800 system and the plasma enhanced chemical vapor deposition (PECVD) Plasmatherm 790 system, resulting in five different SPR chips (Fig. 2). First, BK7 glass substrates were exposed to piranha solution for 30 min at 90 °C (Caution!), and then copiously rinsed with water before drying at 90 °C. The cleaned substrates were used for the e-beam evaporation of 2 nm chromium as the adhesion-promoting layer followed by 52 ± 3 nm gold or silver as the SPR active layer. The substrates were then rendered hydrophilic with 3–6 nm silicon dioxide (SiO_2) during 1.5 s deposition time at 300 °C. For plasmon-waveguide resonance biosensors, the gold (or silver) evaporation was followed by 1–2 nm chromium deposition. The PECVD step was then applied for 5 min to obtain a 510 ± 5 nm SiO_2 waveguiding layer. The obtained chips were stored under vacuum before use.

2.4. Preparation of lipid vesicle solutions

Vesicle solutions were prepared from stock solutions in chloroform. The appropriate mole percent of each lipid was mixed together in a small vial and then dried with nitrogen to form a dry lipid film. Thereafter the lipid containing vial was placed in a vacuum desiccator for 4 h in order to completely remove all chloroform. The lipid was then resuspended in 20 mM PBS solution (containing 150 mM NaCl; pH 7.4) to a lipid concentration of 1.0 mg/mL. After vigorously vortexing to remove all lipid remnants from the vial wall, the solutions were probe sonicated for 20 min. The resuspended lipids were then centrifuged at 8000 rpm for 6 min to remove any titanium particles from the probe tip during sonication. Then the supernatant was extruded through a polycarbonate filter (100 nm) to produce vesicles of uniform size. Small unilamellar vesicles (SUV) prepared by this method were 125 ± 4 nm in diameter as determined by dynamic light scattering (DLS) using a particle sizing analyzer from Brookhaven Instruments Corp (Holtsville, NY).

2.5. Sensitivity comparison assays

The NanoSPR 6: Model 321 (NanoSPR, Illinois) was used for all SPR measurements. This instrument uses a GaAs semiconductor laser ($\lambda = 650$ nm) and 30-μL dual-channel flow cell for high sensitivity refractive index measurements. All experiments were monitored and characterized using the tracking mode of SPR angular scanning around the minimum angle. Initially, all sensor substrates were rinsed with ethanol and ultra pure water. After drying under a gentle stream of N_2 gas, the sensor substrates were clamped down by a dual-channel flow cell on a high-refractive index prism ($n = 1.610$) for use.

The bulk sensitivity study was carried out using ethanol–water mixtures at concentrations $\leq 40\%$ ethanol to ensure working in the linear range of the relationship with the refractive index change (Supplementary data, Fig. S1). The mixtures refractive indices were determined using an ABBE refractometer. All other SPR spectroscopy experiments used a 20 mM phosphate buffered saline solution (pH 7.4 with 150 mM NaCl) as both a running buffer and dilution buffer. Buffer was run across the surface at a flow rate of 6 mL/h unless otherwise noted. Once PBS solution had established a smooth baseline across both channels on the surface, PC or PC/G_{M1} vesicles (1.0 mg/mL in PBS) were injected across the sensor chip. Instant vesicle fusion on the hydrophilic surface was observed and the membrane-covered surface was allowed to incubate until complete vesicle rupture and bilayer formation (ca. 15 min) and then rinsed with PBS to wash away any non-specifically adsorbed vesicles. For the biomolecular interaction analysis (BIA), cholera toxin (CT, 1–100 μg/mL in PBS) was subsequently injected across the sensing surface and incubated to allow for stable lipid–protein binding. Once a stable signal was observed, the surface was rinsed with PBS again. The bare sensor surface was regenerated by injecting 5% Triton X-100 using a modified protocol from our previous work on calcinated nanoglassy substrates [21]. Once 5% Triton X-100 reached the surface, the flow rate was increased 4 times for 30 s to remove bound protein/membrane from the hydrophilic surface, resulting in a return to the sensor baseline and removal of all bound biomolecules. This process of membrane formation, CT binding, and biomolecule removal with surfactant could be easily repeated for numerous cycles and was repeated for each calibration standard along with each sensor chip.

Surface topography imaging of PWR sensors was achieved using *Dimension 3100* atomic force microscope (AFM) and p–n doped Si tips (*Veeco*). The AFM scanning was realized in tapping mode on three different scan sizes: 20 μm × 20 μm, 700 nm × 700 nm and 300 nm × 300 nm.

3. Results and discussion

3.1. Reflectivity curves and FDTD simulations

Before carrying out the computational modeling of the EM field distribution, experimental reflectivity curves were obtained for the different designs. The curves were then fitted to the theoretical data obtained with FDTD calculations as depicted in Fig. 3, and the actual optical parameters of different materials were extracted for further numerical modeling. The curves reported in Fig. 3 show clearly the major differences between SPR and PWR sensors. First, a relative enhancement in reflectance intensity can be observed in silver-based chips compared to gold-based chips. Secondly, the waveguide sensors (Ag-PWR and Au-PWR) generate a sharp dip in the reflectivity spectrum leading to full-width at half-maximum (FWHM) much lower than conventional SPR substrates (Supplementary Data, Table S1). Consequently, the precision of PWR sensors is improved 6 times as compared to SPR chips, while the use of silver provides 2 times improvement compared to the gold chips. Finally, the deposition of 3–6 nm silicon dioxide on the SPR active metal induces a shift in the resonance angle by 0.56°, but also increases the precision by 40%. This unexpected effect on the precision is mainly due to the increase in reflectance intensity by 54% (Table S1).

Some of the observations drawn from the reflectivity curves are confirmed by 3-D FDTD simulations. Fig. 4 provides important indications on the spatial distribution of the evanescent electromagnetic field through the different layers composing the five chips. This distribution depends on the propagation modes involved in each structure. As the guided mode gains in intensity when it propagates, surface plasmon resonance at the interface of a PWR chip is enhanced. Salamon et al. reported an enhancement of the EM field by 25% compared to the field intensity at the interface silver/SiO_2 [9]. The same comparison in Fig. 4 gives an enhancement by 61%, which is related to the optical properties of the materials used. However, in both values the enhancement is partly due the use of silver metal as shown in Fig. 4. Specifically, the enhancement effect due to the waveguide is relatively low (30–35%), while the enhancement due to the silver layer is about 32% with the metals and optical parameters used here.

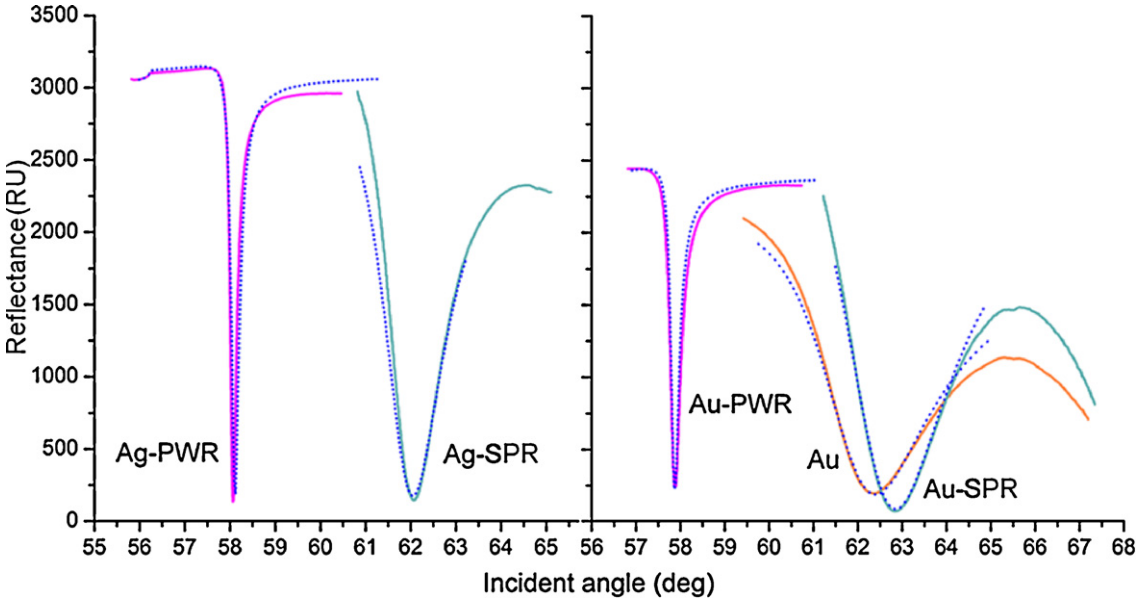

Fig. 3. Reflectance curves obtained with SPR and PWR chips at 650 nm excitation wavelength. The dotted lines represent the fitted theoretical curves. The reflectance is expressed in sensor response unit (RU).

Unlike the field intensity, the penetration depth δ (the distance in the direction perpendicular to the interface at which the EM field intensity decays to $1/e$, 37%) undergoes a significant increase. Fig. 4 shows a value of δ_{PWR} = 828 nm, which is about four times the penetration depth of traditional SPR chips (δ_{SPR} = 216 nm). Apparently, this could be very suitable to studying bacteria (0.5–5.0 μm) and even cells. However, the increase in the penetration depth or electric field intensity does not always lead to improvement in sensitivity as it will be discussed later. Also, the penetration depth at the interface of silver/medium is higher than that at the interface of gold/medium. This is explained by the fact that δ decreases with increasing permittivity of the metal contacting the medium [7].

3.2. Bulk sensitivity assay

Fig. 5 shows the angular bulk sensitivity for the five designs determined by ethanol–water mixtures. For silver-based SPR sensors (Ag–SiO_2-6 nm), a change of 0.01 refractive index units (RIU) induced a shift in the resonance angle by 0.68°, which is 1.8-fold more sensitive than gold-based devices (0.37° for 0.01 RIU). This improvement is the result of the concurrent effect of SPR field enhancement (+30%) discussed previously and the increase in the penetration depth. The latter is likely to play an important role in reducing the effect of diffusion-limited phenomena by expanding the sensing area.

The sensitivity of bare gold substrates is relatively the same to that of the chips functionalized with 3–6 nm SiO_2, indicating that thin films of silicon dioxide has no significant effect on the sensor sensitivity. For a SiO_2 film thickness of ca. 510 nm corresponding to PWR sensors, a decrease in sensitivity by 50% (0.32° per 0.01 RIU for Ag-PWR) was observed. This decrease is in agreement with the theoretical predictions reported by Chien and Chen [22], even though the experimental value found here is much lower than the 10 times decrease predicted in the aforementioned work. However,

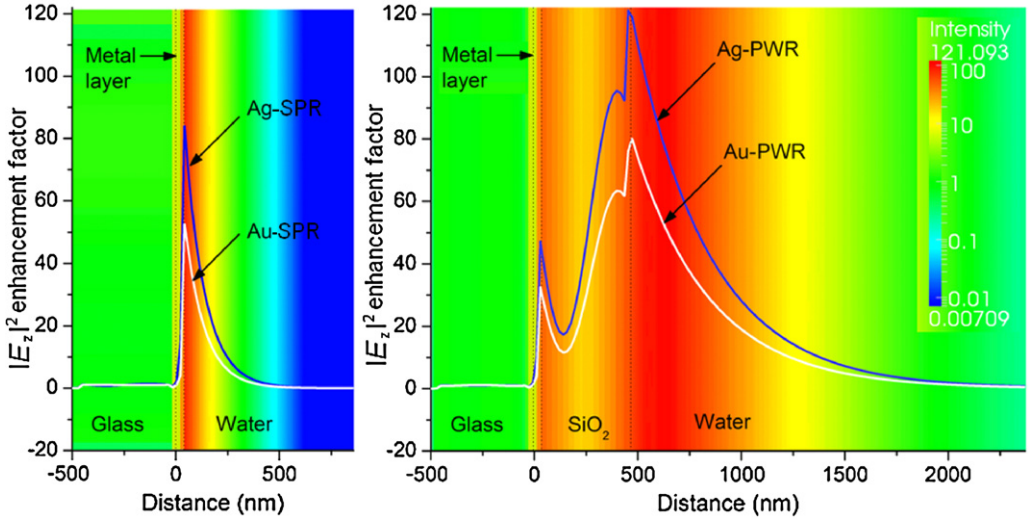

Fig. 4. Spatial distribution of the electric field through the multilayer SPR and PWR chips. The colored background represents the images obtained by 3-D FDTD simulation of Au-SPR and Au-PWR chips at their maximum resonance angle of 62.9° and 58.2° respectively in Kretschmann configuration. The excitation wavelength is 650 nm and the field is unity in the glass substrate.

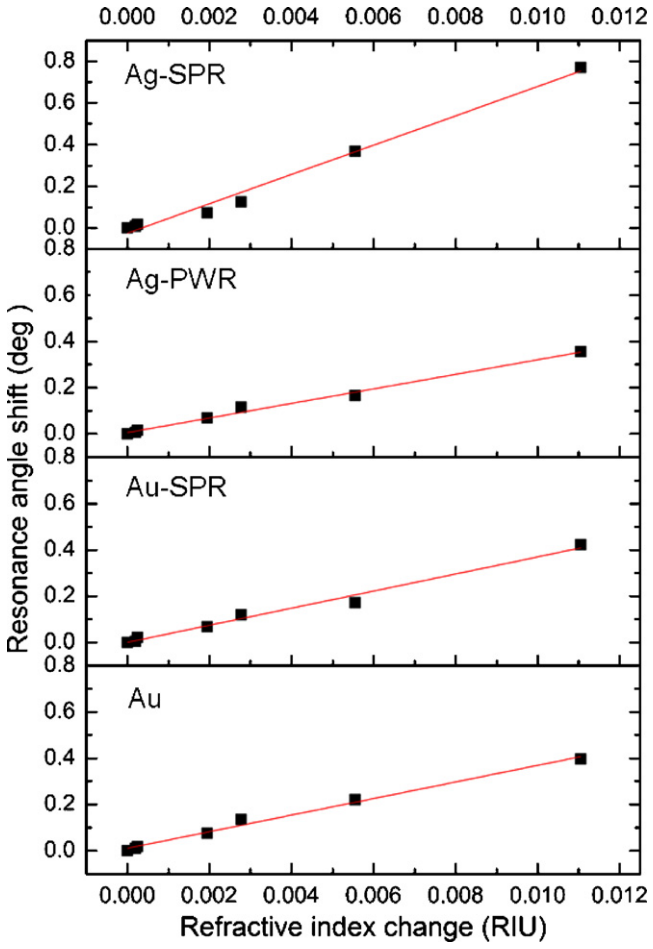

Fig. 5. Bulk sensitivity calibration curves of SPR and PWR sensors obtained by plotting the shift in the resonance angle as a function of the refractive index changes for ethanol–water mixtures.

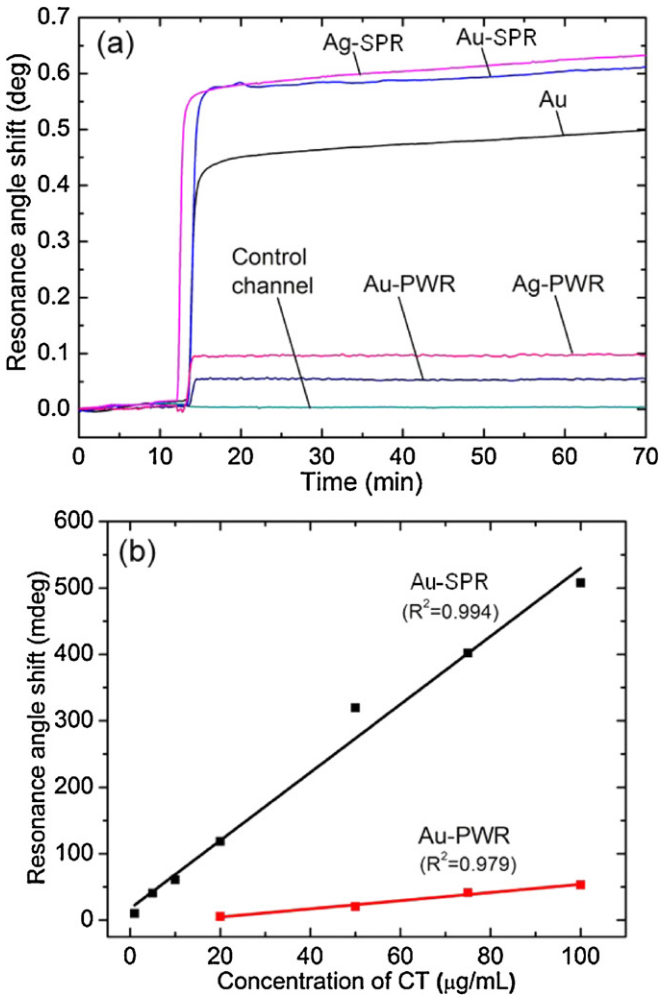

Fig. 6. Surface sensitivity of different SPR and PWR sensor designs. (a) Thickness sensitivity obtained by lipid vesicle fusion on the surface of the different sensors. The control channel only contains PBS solution and serves to monitor the noise and signal drift due to the instrument. (b) Sensitivity to changes in mass for gold-based SPR and PWR biosensors. The calibration curves were obtained for CT-G_{M1} biomolecular interaction.

this result is in opposition to the increase in the EM field intensity in PWR sensors demonstrated previously by FDTD simulations. This apparent discrepancy is less pronounced in the case of the surface sensitivity as discussed below.

3.3. *Surface sensitivity assay*

Since the sensitivity of SPR sensors is due to exponentially decaying evanescent fields, it is important to distinguish the surface sensitivity at the nanometric vicinity of the metal layer from the bulk sensitivity in the surrounding medium. Also, the surface sensitivity should be defined for both thickness variation and mass changes. A change in thickness does not necessarily imply a change in mass (e.g. film polymer swelling/shrinking). Thus, both parameters could independently and differently affect the refractive index of the medium leading to different values of the surface sensitivity. The surface sensitivity study was conducted for both thickness sensitivity and biomolecular interaction analysis, which corresponds to mass change sensitivity. The investigation of the thickness sensitivity is carried out by vesicle fusion and the formation of a 5 nm thick lipid bilayer membrane on SiO_2 functionalized SPR substrates (Fig. 6a). Bare gold substrates are used in this experiment as a control for unfused lipid vesicles and thus will not be used for sensitivity comparison. The SPR chips functionalized with 3–6 nm SiO_2 using either gold or silver present relatively the same thickness sensitivity of 0.120° nm^{-1}. This value falls to 0.010° nm^{-1} and 0.018° nm^{-1} for Au-PWR and Ag-PWR respectively, which is in agreement with the values reported in literature for a lipid bilayer membrane [9]. These results indicate a 6-fold decrease in the surface sensitivity compared to conventional SPR chips. The decrease in surface sensitivity compared to the bulk sensitivity could be explained by the distribution of the SPR evanescent field. In fact, the increase in the penetration depth also means that the surface plasmon polaritons are less bounded to the SiO_2–medium interface because of the higher refractive index of SiO_2 compared to metals, and thus the EM field is less confined to the interface. As a result, the surface sensitivity is highly affected. Additionally, since the decrease rate of the evanescent field is higher in SPR chips than in PWR chips, the bulk sensitivity of both designs become close as we go far from the interface at which the EM field was generated, which explains why the bulk sensitivity is less affected. At a distance over 200 nm, the performance of PWR sensors is expected to be better than conventional SPR sensors.

Another important factor to be considered in the sensitivity decrease in PWR sensors is the surface roughness. Silicon dioxide prepared by PECVD generally exhibits a flat surface with low root mean square (RMS) roughness (<3 nm). However, the increase in thickness of plasma deposited films is known to increase the film surface roughness [23]. The AFM analysis of the surface topography of SiO_2 functionalized PWR sensors indicates an RMS roughness of

1.32 ± 0.05 nm at 700 nm × 700 nm scan size. However, the peak-to-valley surface roughness can reach a value of 10 nm (average height of ~4.3 nm) for the same scan area (Supplementary Data, Fig. S2), which can cause multiple light scattering effects from the arbitrarily rough surface [24] and thus affect the sensitivity [25].

Besides the thickness sensitivity, a biomolecular interaction was carried out (Fig. 6b). The results reveal that the sensitivity of the Au–SiO_2 for the CT/G_{M1} interaction is 5.12 mdeg/(μg/mL), eight times greater than that of the Au-PWR chip for the same interaction (0.62 mdeg/(μg/mL)). However, the gap between SPR and PWR sensitivities to mass changes (biomolecular interactions) is relatively smaller than that obtained for thickness sensitivity. This can be explained by the limitation to CT molecule diffusion before reaching the surface of SPR sensors, while PWR chips are less affected by this phenomenon due to the high penetration depth as discussed previously. Also, the limit of detection (LOD) as determined by the 3σ convention (3 times the standard deviation) for the Au–SiO_2 chips is 6.9 nM compared to 57.2 nM for Au-PWR. This significant increase (about 8-fold) in LOD confirms the general decrease in surface sensitivity as reported above.

The theoretical and experimental results reported in this study point out some causes of the limitations in PWR biosensors. Following the discussion above, an efficient and optimal exploitation of the waveguide mode in PWR sensing may rest on three possible developments: (1) For thin film and lipid bilayer membrane-based analyses, a high penetration depth is not required. Hence new designs could be developed to increase the surface sensitivity by reducing the penetration depth while increasing or keeping unchanged the evanescent field intensity. Preliminary simulations show that these requirements could be satisfied by a simple deposition of a thin gold film on top of the SiO_2 waveguiding layer (Supplementary data, Fig. S3). (2) The surface of PWR sensors could be nanostructured to generate new coupling with localized surface plasmon resonance or to affect the refractive index value at the interface and thus change the evanescent field properties. This strategy has been recently applied for conventional SPR chips by Kabashin et al. [26]. (3) The development of smooth materials or addition of roughness diminishing layers, which has already proven to significantly improve the sensitivity [27,28]. This is crucial to PWR chips because of the accumulation effect of the roughness of different layers. These developments will certainly open new avenues for plasmon-waveguide resonance biosensors.

4. Conclusion

We have reported the sensitivity comparison of SPR and PWR biosensors for both gold and silver-based substrates. The use of a waveguide layer significantly increases the penetration depth and improves the resolution. However, loss of the surface sensitivity is observed for both thickness and mass changes. In addition, the sensitivity to refractive index changes in the bulk solution is affected. It is pertinent to point out that these parameters are differently affected by the addition of the waveguide layer, depending on the specific experiment and the considered interaction. Unlike SPR chips, the high penetration depth in PWR sensors tends to diminish the limitations caused by diffusion phenomena and thus largely retains the bulk sensitivity. On the other hand, the high penetration depth also means minimal confinement of the evanescent electric field at the interface, leading to decreased surface sensitivity.

Considering the experimental results presented here and the related biosensing studies reported in literature, it appears that PWR biosensors could be useful and instructive as a qualitative informational platform for anisotropic materials or for the monitoring of small cells, viruses and bacteria. Also, for targets lying at distances higher than 200 nm from the interface or for events occurring in the direction perpendicular to the interface, PWR sensors can be a very interesting alternative. The ability to probe events by using s-polarized light is particularly attractive in this case. However, the current study demonstrates that traditional PWR sensors with a simple dielectric slab waveguide are less suitable for high sensitivity measurements, especially for those occurring at the nanometer vicinity of the interface. To raise the surface sensitivity of PWR platforms to the expectations and promise drawn by the waveguide theory, new designs and concepts need to be developed.

Acknowledgments

The authors gratefully acknowledge the financial support of the US National Science Foundation (CHE-0719224) and the National Institute of Health (1R21EB-009551). The authors also thank Dr. Scott Saavedra for helpful discussion.

Appendix A. Supplementary data

Supplementary data associated with this article can be found, in the online version, at doi:10.1016/j.snb.2011.04.008.

References

[1] L.K. Gifford, I.E. Sendroiu, R.M. Corn, A. Luptak, J. Am. Chem. Soc. 132 (2010) 9265–9267.
[2] Y. Liu, Y. Dong, J. Jauw, M.J. Linman, Q. Cheng, Anal. Chem. 82 (2010) 3679–3685.
[3] Y. Liu, P.H. Liao, Q.A. Cheng, R.J. Hooley, J. Am. Chem. Soc. 132 (2010) 10383–10390.
[4] J.S. Mitchell, Y. Wu, Methods Mol. Biol. 627 (2010) 113–129.
[5] K.M. Mayer, F. Hao, S. Lee, P. Nordlander, J.H. Hafner, Nanotechnology 21 (2010) 255503.
[6] S. Wang, X. Shan, U. Patel, X. Huang, J. Lu, J. Li, N. Tao, Proc. Natl. Acad. Sci. U.S.A. 107 (2010) 16028–16032.
[7] A. Abbas, M.J. Linman, Q. Cheng, Biosens. Bioelectron. 26 (2011) 1815–1824.
[8] H.A. Macleod (Ed.), Thin Films Optical Filters, Hilger, Bristol, and Macmillan, NewYork, 1986.
[9] Z. Salamon, H.A. Macleod, G. Tollin, Biophys. J. 73 (1997) 2791–2797.
[10] Z. Salamon, G. Tollin, Spectroscopy 15 (2001) 161–175.
[11] S. Toyama, N. Doumae, A. Shoji, Y. Ikariyama, Sens. Actuator B: Chem. 65 (2000) 32–34.
[12] H. Zhang, K.S. Orosz, H. Takahashi, S.S. Saavedra, Appl. Spectrosc. 63 (2009) 1062–1067.
[13] M. Zourob, N.J. Goddard, Biosens. Bioelectron. 20 (2005) 1718–1727.
[14] M. Zourob, S. Mohr, B.J.T. Brown, P.R. Fielden, M.B. McDonnell, N.J. Goddard, Lab Chip 5 (2005) 1360–1365.
[15] V.J. Hruby, I. Alves, S. Cowell, Z. Salamon, G. Tollin, Life Sci. 86 (2010) 569–574.
[16] V.J. Hruby, G. Tollin, Curr. Opin. Pharmacol. 7 (2007) 507–514.
[17] M. Zourob, J.J. Hawkes, W.T. Coakley, B.J.T. Brown, P.R. Fielden, M.B. McDonnell, N.J. Goddard, Anal. Chem. 77 (2005) 6163–6168.
[18] P.K. Tien, Rev. Mod. Phys. 49 (1977) 361.
[19] K.H.A. Lau, L.S. Tan, K. Tamada, M.S. Sander, W. Knoll, J. Phys. Chem. B 108 (2004) 10812–10818.
[20] D.G. Zhang, K.J. Moh, X.C. Yuan, Opt. Express 18 (2010) 12185–12190.
[21] M.J. Linman, S.P. Culver, Q. Cheng, Langmuir 25 (2009) 3075–3082.
[22] F.C. Chien, S.J. Chen, Biosens. Bioelectron. 20 (2004) 633–642.
[23] D.M. Tanenbaum, A.L. Laracuente, A. Gallagher, Phys. Rev. B 56 (1997) 4243.
[24] H. Raether, Surface Plasmons on Smooth and Rough Surfaces and on Grattings, Springer-Verlag, Berlin, 1988.
[25] T. Velinov, L. Ahtapodov, A. Nelson, M. Gateshki, M. Bivolarska, Thin Solid Films 519 (2011) 2093–2097.
[26] A.V. Kabashin, P. Evans, S. Pastkovsky, W. Hendren, G.A. Wurtz, R. Atkinson, R. Pollard, V.A. Podolskiy, A.V. Zayats, Nat. Mater. 8 (2009) 867–871.
[27] X. Chen, M. Pan, K. Jiang, Microelectron. Eng. 87 (2010) 790–792.
[28] H. Liu, B. Wang, E.S.P. Leong, P. Yang, Y. Zong, G. Si, J. Teng, S.A. Maier, ACS Nano 4 (2010) 3139–3146.

Biographies

Abdennour Abbas received his M.S. degree in Physical Chemistry of Biological Systems in 2006 and his Ph.D. degree in Materials Science and Engineering in October 2009 from the Scientific and Technology University of Lille in France. His first

postdoctoral research at the University of California Riverside was dedicated to the development of novel biochips for SPR spectroscopy and imaging. Early this year (2011), he joined the Department of Mechanical Engineering and Materials Science at Washington University in St Louis where he is investigating new plasmonic nanostructure-based biosensors for LSPR and SERS detection. His research interests are in optical biosensors, bioMEMS, micro/nanofabrication, plasmonic nanostructures, biointerfaces, and advanced materials for micro/nanotechnology and bioengineering.

Matthew J. Linman is a recent Ph.D. graduate from Dr. Quan Cheng's lab at UC Riverside. He received his BA degree in chemistry from The College of Wooster in Wooster, Ohio in 2005. His doctoral research mainly focused on the development of effective biointerfaces and novel biomaterials for biosensing applications with surface plasmon resonance spectroscopy and the associated technique of SPR imaging.

Quan "Jason" Cheng received his BS and MS degree in chemistry from Nanjing University, China, and Ph.D. degree in analytical chemistry from the University of Florida in 1995. After a postdoctoral stint at University of California at Berkeley, he took a staff scientist position in 1997 at Lawrence Berkeley National Laboratory and later became a group leader. He joined the chemistry faculty of the University of California at Riverside as an assistant professor in 2001, and was promoted to associate professor in 2007 and full professor in 2010. His research interests include functional materials and biosensing technologies with surface plasmon resonance, microarray, electrochemistry, and surface-enhanced mass spectrometric methods.